Article citation info:
Lipski A., Karolewski S. 2025. Strength of High-Density Wood-Based Panels Reinforced with Melamine Films. *Drewno. Prace naukowe. Doniesienia. Komunikaty* 68 (215): 00048. https://doi.org/10.53502/wood-200039

Łukasiewicz Poznań Institute of Technology

Drewno. Prace naukowe. Doniesienia. Komunikaty
Wood. Research papers. Reports. Announcements

Journal website: https://drewno-wood.pl

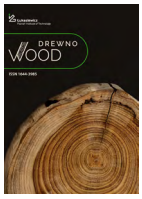

Strength of High-Density Wood-Based Panels Reinforced with Melamine Films

Adam Lipski[a] *
Sebastian Karolewski[b]

[a] Laboratory for Research on Materials and Structures, Bydgoszcz University of Science and Technology, Poland, Bydgoszcz, Poland
[b] Doctoral School, Bydgoszcz University of Science and Technology, Bydgoszcz, Poland

Article info
Received: 25 May 2024
Accepted: 13 January 2025
Published: 18 March 2025

Keywords
high-density fiberboard
high-density wood-based panel
melamine film reinforcement
tensile test
ANOVA

Wood-based panels are a group of products with a wide range of applications. They are not obtained from solid wood, but are made from wood fragments, such as wood chips, sawdust or wood dust, which are usually waste from production. The recycled material, after being mixed with a binder, is compressed. As a consequence of such a process, different types of boards are obtained: MDF (Medium-Density Fiberboard), HDF (High-Density Fiberboard), fiberboard or particleboard. In response to the problems accompanying the use of MDF and HDF boards, a new type of wood-based boards has been developed, called CDF (Compact Density Fiberboard).

In this study the strength properties of CDF panels reinforced with melamine films were investigated for four thicknesses: 6.4 mm, 8.4 mm, 10.4 mm and 12.4 mm. Young's modulus E, tensile strength Rm and percentage total extension at fracture At were determined by a static tensile test. The results of the strength tests of wood-based panels were subjected to statistical analysis to determine the effect of the thickness of the panel on its strength.

CDF boards have a low total elongation at break of about 0.5%, and exhibit greater stiffness, with a Young's modulus of at least 5,600 MPa. The statistical analysis shows that for boards up to 12.4 mm thick, their thickness usually does not affect the strength properties. The only exception is in the Young's modulus values for a thickness of 12.4 mm.

DOI: 10.53502/wood-200039

Introduction

Wood-based panels are a group of products with a wide range of applications, obtained not from solid wood, but from wood fragments. Wood-based panels are produced by defibering wood into wood fiber, which is mixed with waxes or synthetic resins, such as urea–formaldehyde resin, and pressed under high pressure and temperature (Roila, 2023). The raw material used to produce wood-based panels consists mainly of shavings, sawdust, plywood strips, small wood particles, and chips (Kim and Song, 2014). In the production of wood panels, various types of additives can be used, often recycled, to improve their properties; for example, kenaf, wheat straw, Californian pine, bamboo, as well as other types of fibers, not necessarily wood fibers (Roila, 2023). In addition, rubber wood can be successfully used in production, although due to climate change in the form of prolonged wet periods, especially on high slopes, the extraction of this raw material has

* Corresponding author: adlippkm@pbs.edu.pl

become inefficient (Rowson, 2022). There are a number of scientific publications describing the process of manufacturing wood-based panels using waste material, which is beneficial from the point of view of environmental protection (Onisko, 2011). However, unlike primary raw materials, recycled materials exhibit inferior physicochemical properties (Lubis et al., 2018), which may affect the properties of the finished panels (Zhao et al., 2019). There are existing works describing hardboards made of recycled corrugated cardboard (Hunt et al., 1999). MDF boards can be made exclusively from waste material, as well as from recovered newspaper fibers (Nourbakhsh et al., 2010). Waste from HDF boards can also be reused in the production of high-density fiberboards. In 2020, results were published from research on the effect of adding waste on the properties of high-density fiber composites. In some cases, adding recycled HDF board had a beneficial effect on the properties of the final product. In this case, a 30% reduction in water absorption and a 12% lower surface roughness were observed (Sala, 2020). The subject literature also contains research on wood-based boards with melamine admixtures. Lieber et al. (2018) analyzed the effect of the seasoning period of particleboards containing melamine–urea–formaldehyde resin on their mechanical properties. In 2019, the results of a study on the effect of conditions of use on selected properties of furniture particleboards finished with a melamine film were published (Borysiuk et al., 2019). Melamine additives can be used in the production of wood-based panels in various amounts. Franco et al. (2024) investigated the effect of adding melamine paper shavings (0%, 5%, 10%) in the production of MDF panels. Through this process, different types of boards are obtained: MDF (Medium-Density Fiberboard), HDF (High-Density Fiberboard), fiberboard, and particleboard.

The currently used HDF or MDF boards have relatively high price and moderate durability. HDF boards are primarily designed to produce floor panels, and are less commonly used in the furniture industry. To produce furniture, MDF boards are commonly used – in Poland the standard thickness is 18 mm (Sydor and Wołpiuk, 2016), which leads to inefficient use of available space. Boards exposed to water swell, deform, and consequently lose their properties. If exposed to open flames, they quickly become charred. HDF and MDF boards generate high production costs and create many operational problems.

In response to the problems accompanying the use of MDF and HDF boards, a new type of wood-based boards, called SwissCDF, has been developed by Swiss Krono (Swiss Krono, 2023). These are black-stained, refined HDF wood-based boards pressed under high pressure, which gives them a high density of over 1000 kg/m^3. The surface of the boards is protected by multiple layers of melamine film coating, making them highly stable and resistant to scratches, water splashes and even fire. CDF (Compact Density Fiberboard) is particularly recommended as a structural element of luxury furniture, which requires above-average strength and the highest quality of workmanship. The increased moisture resistance of CDF boards makes them ideal for use in furniture for rooms with increased humidity, such as bathroom cabinets or furniture for wellness zones. These boards have a limited formaldehyde content (≤ 8 mg per 100 g dry weight). In case of contact with an open source of fire, they achieve a flame retardancy of C-s2, d0 class. These boards are produced with thicknesses ranging from 6.4 to 19.4 mm.

Tests conducted by the manufacturer have shown that for unlaminated, raw CDF boards with thicknesses of 5.8 mm, 7.8 mm, 9.8 mm and 11.8 mm, the bending strength measured according to the EN 310 standard exceeds 60 MPa. For comparison, the value of this parameter is in the range 17–23 MPa for MDF boards, and is 40 MPa for HDF boards. In addition, CDF boards have a modulus of elasticity in bending in the range 5500–6000 MPa, depending on the thickness. The minimum transverse tensile strength is 1.8–2.0 MPa. The manufacturer also declares a peel strength (glued joint) of > 1.8 MPa for boards with a thickness of 15.8 mm and 18.8 mm and > 2.0 MPa for boards with a thickness of 5.8–11.8 mm (SwissKrono. Product card).

In the present study, the strength properties of CDF panels reinforced with melamine films were investigated for four thicknesses: 6.4 mm, 8.4 mm, 10.4 mm, and 12.4 mm. Young's modulus E, tensile strength R_m and total elongation at break A_t were determined by a static tensile test. Based on statistical analysis of the results, the research hypothesis regarding the effect of the thickness of a CDF wood-based board on its strength properties under tensile load was verified.

Materials and methods

The research material consisted of commercial Swiss-CDF wood-based boards with thicknesses of 6.4 mm, 8.4 mm, 10.4 mm and 12.4 mm, coated on both sides with a cellulose laminate with an admixture of epoxy resin. The core of the tested CDF board was made of crushed, colored wood material, which was additionally reinforced with a two-layer melamine film. Due to the presence of melamine and the high forming pressure, the CDF board is flame retardant and resistant to external factors, including water. The boards were supplied by an external supplier, and the shaped test specimens were made at the research unit.

Tests were carried out on type A universal samples made in accordance with PN-EN ISO 3167:2014-09

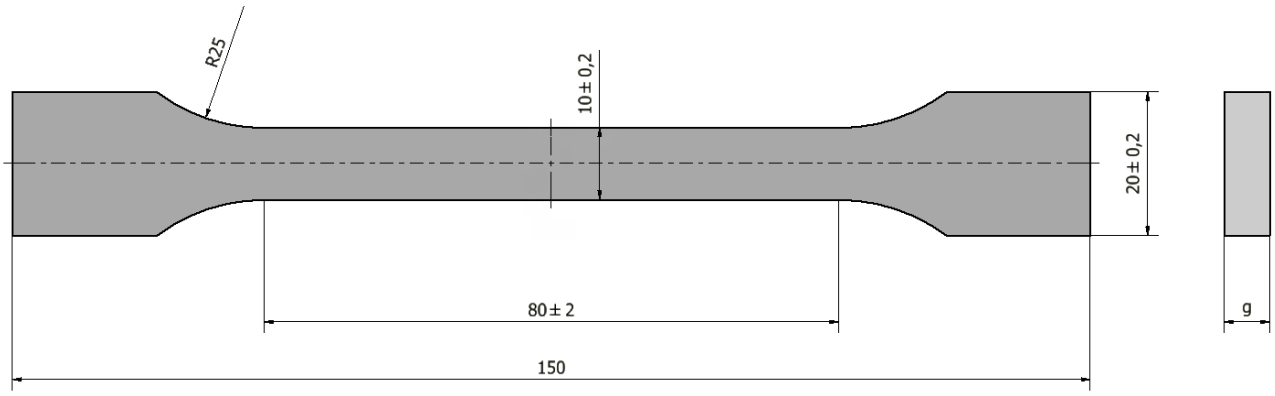

Fig. 1. Dimensions of a test specimen. The thickness g of the specimen corresponds to the thickness of the tested panel

(Fig. 1). The thickness *g* of the samples corresponded to the thickness of the boards from which the samples were made (6.4 mm, 8.4 mm, 10.4 mm or 12.4 mm). Three samples were tested for each thickness of CDF board.

The results of thickness and width measurements of specimens, used to determine the initial cross-section, along with determined measurement uncertainty (Arendarski, 2013; Kostyrko and Piotrowski, 2012), are shown in Table 1 and Table 2. The following designations are used in the table:

g_1, g_2, g_3 – individual sample thickness measurements in the measured section, mm;

b_1, b_2, b_3 – individual sample width measurements in the measured section, mm;

g_0, b_0 – average thickness or average width of the sample in the measured section, mm;

s_x – standard deviation of sample thickness or width in the measured section, mm.

Type A uncertainty was determined for the thickness g_0 or width b_0 of individual samples assuming that the measurement results have a normal distribution:

$$u_{x(A)} = \frac{s_x}{\sqrt{n}} \tag{1}$$

where n is the number of measurements and s_x is the standard deviation for the dimension in question.

Type B uncertainty was determined for a measurement with a digital micrometer with an elementary plot of $\Delta x = 0.01$ mm assuming a uniform probability distribution:

$$u_{x(B)} = \frac{\Delta x}{\sqrt{3}} \tag{2}$$

The total uncertainty of the thickness or width measurements of the samples was determined based on the relationship

$$u_{x(C)} = \sqrt{\left(u_{x(A)}\right)^2 + \left(u_{x(B)}\right)^2} \tag{3}$$

The expanded uncertainty of the measurements was determined by assuming a coverage factor of $k = 2$ (a confidence level of about 95%):

$$U_x = k \cdot u_{x(C)} \tag{4}$$

The size of the initial cross-section of the sample S_0 (Table 3) is determined by the formula

$$S_0 = b_0 \cdot g_0 \tag{5}$$

and the compound uncertainty of the measurement of the cross-sectional relationship is

$$u_{S_0} = \sqrt{\left(\frac{\partial S_0}{\partial b}\right)^2 \cdot u_b^2 + \left(\frac{\partial S_0}{\partial g}\right)^2 \cdot u_g^2} \tag{6}$$

where:

b_0, g_0 – denote the initial width and initial thickness, respectively, of the individual samples in the measured section, mm;

u_b, u_g – denote the uncertainty of the measurement of the width and thickness, respectively, of the individual samples in the measured section.

Since

$$\frac{\partial S_0}{\partial b} = g_0 \tag{7}$$

and

$$\frac{\partial S_0}{\partial g} = b_0 \tag{8}$$

we have

$$u_{S_0} = \sqrt{g_0 \cdot u_b^2 + b_0 \cdot u_g^2} \tag{9}$$

Table 1. Results of thickness measurements of specimens g_0 with the measurement uncertainty (expansion coefficient k = 2)

Nominal thickness	Sample designation	g_1	g_2	g_3	g_0	s_x	$u_{x(A)}$	$u_{x(B)}$	$u_{x(C)}$	$g_0 \pm U_x$
		mm								
6.4 mm	6-1	6.31	6.32	6.32	6.32	0.01	0.01		0.01	6.32 ± 0.02
	6-2	6.28	6.29	6.29	6.29	0.01	0.01		0.01	6.29 ± 0.02
	6-3	6.36	6.36	6.36	6.36	0.01	0.01		0.01	6.36 ± 0.02
8.4 mm	8-1	8.44	8.44	8.44	8.44	0.00	0.00		0.01	8.44 ± 0.02
	8-2	8.45	8.39	8.43	8.42	0.03	0.02		0.02	8.42 ± 0.04
	8-3	8.43	8.38	8.43	8.41	0.03	0.02	0.01	0.02	8.41 ± 0.04
10.4 mm	10-1	10.40	10.44	10.43	10.42	0.02	0.01		0.01	10.42 ± 0.02
	10-2	10.43	10.40	10.44	10.42	0.02	0.01		0.01	10.42 ± 0.02
	10-3	10.44	10.41	10.44	10.43	0.02	0.01		0.01	10.43 ± 0.02
12.4 mm	12-1	12.20	12.20	12.20	12.20	0.00	0.00		0.01	12.20 ± 0.02
	12-2	12.20	12.20	12.20	12.20	0.00	0.00		0.01	12.20 ± 0.02
	12-3	12.00	12.00	12.00	12.00	0.00	0.00		0.01	12.00 ± 0.02

Table 2. Results of width measurements of specimens b_0 with the measurement uncertainty (expansion coefficient k = 2)

Nominal thickness	Sample designation	b_1	b_2	b_3	b_0	s_x	$u_{x(A)}$	$u_{x(B)}$	$u_{x(C)}$	$b_0 \pm U_x$
		mm								
6,4 mm	6-1	10.30	10.30	10.48	10.36	0.10	0.06		0.06	10.36 ± 0.12
	6-2	10.30	9.85	10.33	10.16	0.27	0.16		0.16	10.16 ± 0.31
	6-3	10.29	10.24	10.69	10.41	0.25	0.14		0.14	10.41 ± 0.29
8,4 mm	8-1	10.23	9.89	10.52	10.21	0.32	0.18		0.18	10.21 ± 0.37
	8-2	10.01	9.95	10.60	10.19	0.36	0.21		0.21	10.19 ± 0.42
	8-3	10.10	9.95	10.44	10.16	0.25	0.14		0.14	10.16 ± 0.29
10,4 mm	10-1	10.85	10.40	10.60	10.62	0.23	0.13	0.01	0.13	10.62 ± 0.27
	10-2	10.29	10.10	10.07	10.15	0.12	0.07		0.07	10.15 ± 0.14
	10-3	10.36	10.07	10.23	10.22	0.15	0.09		0.09	10.22 ± 0.17
12,4 mm	12-1	10.18	10.55	12.30	10.34	0.19	0.11		0.11	10.34 ± 0.22
	12-2	10.70	10.30	10.58	10.53	0.21	0.12		0.12	10.53 ± 0.24
	12-3	10.10	9.90	10.10	10.03	0.12	0.07		0.07	10.03 ± 0.14

Table 3. Cross-section S_0 of samples with the measurement uncertainty (expansion coefficient k = 2)

Nominal thickness	Sample designation	Specimen thickness	Specimen width	Sample cross-section
		g_0, mm	b_0, mm	S_0, mm²
6.4 mm	6-1	6.32 ± 0.02	10.36 ± 0.15	65.5 ± 4.0
	6-2	6.29 ± 0.02	10.16 ± 0.41	63.9 ± 6.0
	6-3	6.36 ± 0.01	10.41 ± 0.38	66.2 ± 5.8
8.4 mm	8-1	8.44 ± 0.01	10.21 ± 0.49	86.2 ± 8.5
	8-2	8.45 ± 0.08	10.19 ± 0.55	86.1 ± 9.7
	8-3	8.41 ± 0.06	10.16 ± 0.38	85.5 ± 8.2
10.4 mm	10-1	10.42 ± 0.05	10.62 ± 0.35	110.7 ± 9.3
	10-2	10.42 ± 0.03	10.15 ± 0.18	105.8 ± 6.8
	10-3	10.43 ± 0.03	10.22 ± 0.23	106.6 ± 7.5
12.4 mm	12-1	12.20 ± 0.01	10.01 ± 0.20	122.1 ± 7.8
	12-2	12.20 ± 0.01	10.53 ± 0.32	128.5 ± 9.9
	12-3	12.00 ± 0.01	10.03 ± 0.18	120.4 ± 7.4

The expanded uncertainty of the initial cross-section of the sample S_0 was determined analogously to equation (4) by assuming a coverage factor of $k = 2$ (a confidence level of about 95%).

Tensile tests were carried out in accordance with PN-EN ISO 527-2:2012 using an INSTRON 5966 testing machine. The specimens, axially fixed in the machine's grips (Fig. 2), were subjected to monotonically increasing tensile loading, with the testing machine's piston travel speed set at 0.05 mm/s. The tests were conducted at a temperature of 21 °C and a humidity of 45%. During the test, the actual values of the loading force, the displacement of the grip of the testing machine, and the deformation of the specimen in the measurement section were recorded using an extensometer with a measuring base of 50 mm and a measuring range of ±5 mm. The tests were continued until the specimen broke.

The stress in the measured part of a tensile specimen is determined by the formula

$$\sigma = \frac{F}{S_0} \tag{10}$$

and the compound uncertainty of the stress measurement is

$$u_\sigma = \sqrt{\left(\frac{\partial\sigma}{\partial F}\right)^2 \cdot u_F^2 + \left(\frac{\partial\sigma}{\partial S_0}\right)^2 \cdot u_{S_0}^2} \tag{11}$$

where:
F is the tensile force, N;
S_0 is the initial cross-section of the sample, mm²;
u_F is the uncertainty of the force measurement, N;
u_{S_0} is the uncertainty of the measurement of the initial cross-section of the sample, mm².

Since

$$\frac{\partial\sigma}{\partial F} = \frac{1}{S_0} \tag{12}$$

and

$$\frac{\partial\sigma}{\partial S_0} = -\frac{F}{S_0^2} \tag{13}$$

we have

$$u_\sigma = \sqrt{\left(\frac{1}{S_0}\right)^2 \cdot u_F^2 + \left(\frac{F}{S_0^2}\right)^2 \cdot u_{S_0}^2} \tag{14}$$

The expanded uncertainty (equation 14) of the tensile strength R_m was determined analogously to equation (4) by assuming a coverage factor of $k = 2$ (a confidence level of about 95%).

The uncertainty of the force measurement was determined based on the load cell class of the testing machine (K = 0.5) and its measurement range of ΔF = 10 kN:

Fig. 2. Specimen in the jaws of an INSTRON 5699 testing machine with extensometer attached

$$u_F = \frac{K \cdot \Delta F}{100} = 50\ N \tag{15}$$

The uncertainty of the strain measurement was determined by the class of the extensometer (K = 0.5), its measurement range Δe = 5 mm, and the base L_0 = 50 mm, i.e. Δε = 10%:

$$u_\varepsilon = \frac{K \cdot \Delta\varepsilon}{100} = 0.05\% \tag{16}$$

Young's modulus *E* was determined using a linear regression method for the linear relationship between the force *F* and the strain ε recorded during the test, expressed in mm/mm:

$$E = \frac{F}{S_0 \cdot \varepsilon} = \frac{m_E}{S_0} \tag{17}$$

for which the equation of the regression line takes the form

$$F = m_E \cdot \varepsilon + b_E \tag{18}$$

where is the slope of the regression line and is the intercept of the regression line.

The compound uncertainty of the measurement of Young's modulus is given by

$$u_E = \sqrt{\left(\frac{\partial E}{\partial m_E}\right)^2 \cdot S_{m_E}^2 + \left(\frac{\partial E}{\partial S_0}\right)^2 \cdot u_{S_0}^2} \tag{19}$$

where is the standard deviation of the slope of the regression line.

Because

$$\frac{\partial E}{\partial m_E} = \frac{1}{S_0} \tag{20}$$

and

$$\frac{\partial E}{\partial S_0} = -\frac{m_E}{{S_0}^2} \tag{21}$$

we have

$$u_E = \sqrt{\left(\frac{1}{S_0}\right)^2 \cdot S_{m_E}^2 + \left(\frac{m_E}{{S_0}^2}\right)^2 \cdot u_{S_0}^2} \tag{22}$$

As before, the expanded uncertainty was determined by taking the expansion factor $k = 2$ (a confidence level of about 95%).

The following is the standard deviation of the slope of the regression line (Table 6) for *n* pairs of F_i, ε_i, on the basis of which the regression line was determined:

$$S_{m_E} = \sqrt{\frac{(1 - r^2) \cdot S_F^2}{(n - 2) \cdot S_\varepsilon^2}} \tag{23}$$

where the standard deviation of the force values F_i described by the axis of ordinates is

$$S_F = \sqrt{\frac{1}{n - 1} \cdot \left[\sum_{i=1}^{n} F_i^2 - \frac{(\sum_{i=1}^{n} F_i)^2}{n}\right]} \tag{24}$$

and the standard deviation of strain values ε_i described by the axis of abscissae is

$$S_\varepsilon = \sqrt{\frac{1}{n-1} \cdot \left[\sum_{i=1}^{n} \varepsilon_i^2 - \frac{(\sum_{i=1}^{n} \varepsilon_i)^2}{n} \right]} \quad (25)$$

The coefficient of correlation is

$$r = \frac{S_{\varepsilon F}}{S_\varepsilon \cdot S_F} \quad (26)$$

where the covariance is given by

$$S_{\varepsilon F} = \frac{1}{n-1} \cdot \left[\sum_{i=1}^{n} \varepsilon_i \cdot F_i - \frac{\sum_{i=1}^{n} \varepsilon_i \cdot \sum_{i=1}^{n} F_i}{n} \right] \quad (27)$$

The test results were analyzed to determine the possible effect of CDF plate thickness on the strength properties. Statistical analysis was carried out based on one-way analysis of variance (ANOVA) using the advanced analytics software package STATISTICA (StatSoft, 2006) according to the flow chart shown in Fig. 3 (Rabiej, 2018). One-way ANOVA is a method of testing the results of measurements that are influenced by only one factor, in this case the thickness of the CDF plate.

Results and discussion

The actual values of the loading force recorded during the tests were divided by the initial cross-section S_0 to determine the stress–strain relationship for the specimen in the measurement section (Fig. 4).

Tensile strength R_m, percentage total extension at fracture A_t and Young's modulus E, along with

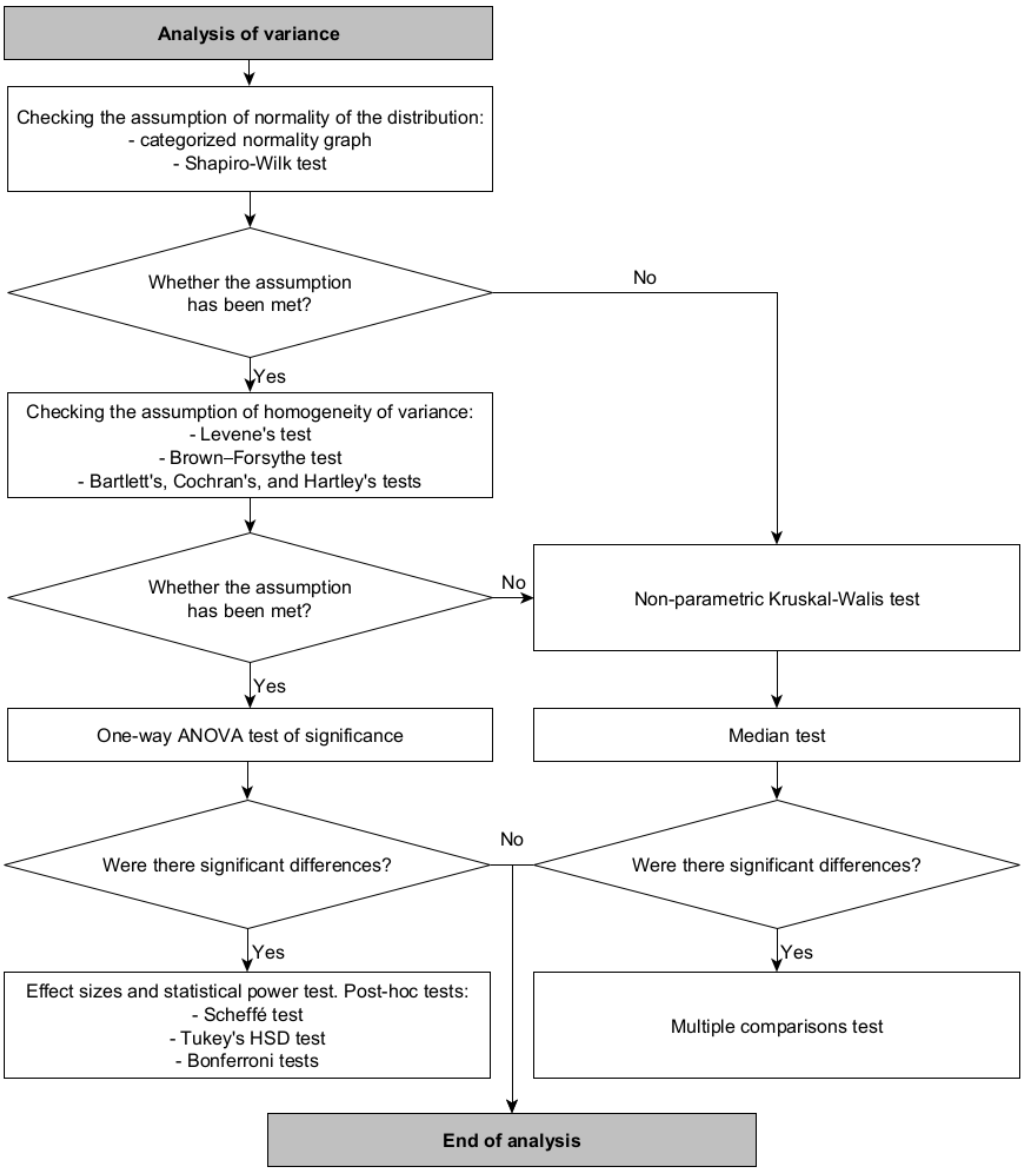

Fig. 3. Flow chart for one-way ANOVA analysis of variance

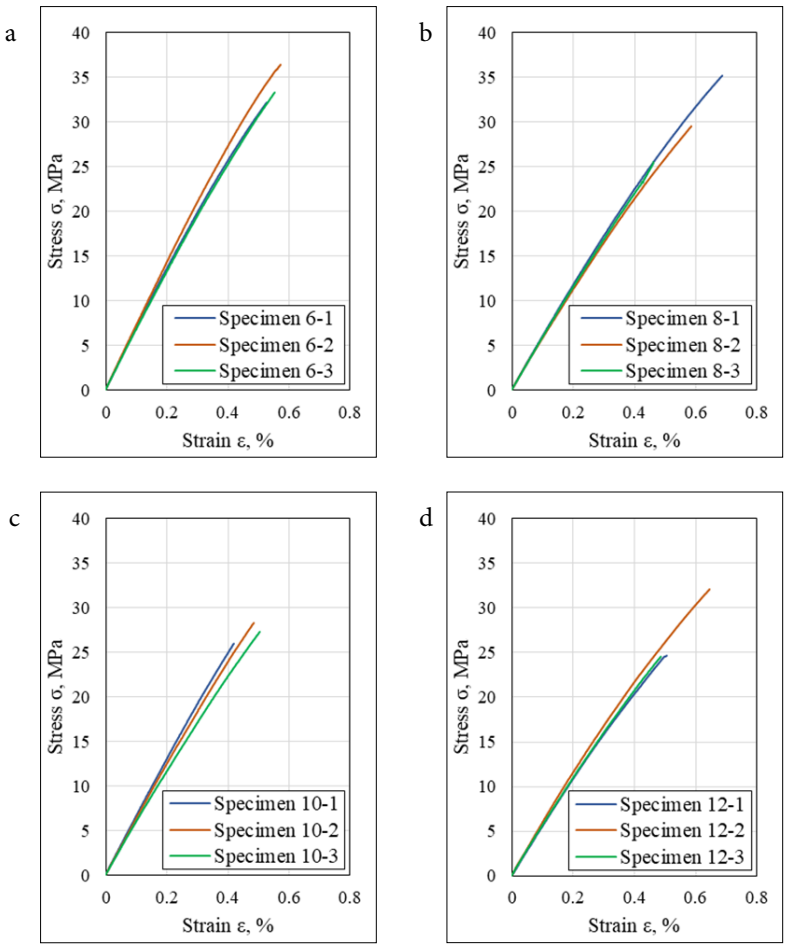

Fig. 4. Tensile test results for different thicknesses of wood-based panels: 6.4 mm (a), 8.4 mm (b), 10.4 mm (c) and 12.4 mm (d)

Table 4. Tensile strength R_m with the measurement uncertainty (expansion coefficient k = 2)

Nominal thickness	Sample designation	F		S_0	u_{S0}	R_m	u_{Rm}	$R_m \pm U_{Rm}$	$R_m \pm U_{Rm}$ (avg.)
		N	N	mm²	mm²	MPa	MPa	MPa	MPa
6.4 mm	6-1	2107.2	50	65.5	1.8	32.2	1.2	32.2 ± 2.3	34.0 ± 3.5
	6-2	2327.7		63.9	2.6	36.4	1.7	36.4 ± 3.4	
	6-3	2204.1		66.2	2.6	33.3	1.5	33.3 ± 3.0	
8.4 mm	8-1	3028.9	50	86.2	3.7	35.1	1.6	35.1 ± 3.2	30.0 ± 3.5
	8-2	2532.9		85.8	4.1	29.5	1.5	29.5 ± 3.0	
	8-3	2180.7		85.4	3.5	25.5	1.2	25.5 ± 2.4	
10.4 mm	10-1	2869.1	50	110.7	4.0	25.9	1.0	25.9 ± 2.1	27.2 ± 2.1
	10-2	2999.3		105.8	3.0	28.3	0.9	28.3 ± 1.9	
	10-3	2909.5		106.6	3.3	27.3	1.0	27.3 ± 1.9	
12.4 mm	12-1	3108.1	50	126.1	4.1	24.6	0.9	24.6 ± 1.8	27.1 ± 2.6
	12-2	4125.9		128.5	4.3	32.1	1.1	32.1 ± 2.3	
	12-3	2960.2		120.4	3.3	24.6	0.8	24.6 ± 1.6	

Table 5. Percentage total extension at fracture A_t with the measurement uncertainty (expansion coefficient k = 2)

Nominal thickness	Sample designation	A_t	u_ε	$A_t \pm U_\varepsilon$	$A_t \pm U_\varepsilon$ (avg.)
		%	%	%	%
6.4 mm	6-1	0.528	0.05	0.528 ± 0.1	0.551 ± 0.14
	6-2	0.573		0.573 ± 0.1	
	6-3	0.552		0.552 ± 0.1	
8.4 mm	8-1	0.685	0.05	0.685 ± 0.1	0.578 ± 0.24
	8-2	0.587		0.587 ± 0.1	
	8-3	0.462		0.462 ± 0.1	
10.4 mm	10-1	0.419	0.05	0.419 ± 0.1	0.469 ± 0.17
	10-2	0.485		0.485 ± 0.1	
	10-3	0.504		0.504 ± 0.1	
12.4 mm	12-1	0.504	0.05	0.504 ± 0.1	0.545 ± 0.22
	12-2	0.645		0.645 ± 0.1	
	12-3	0.487		0.487 ± 0.1	

Table 6. Summary of the parameters used to determine the standard deviation of the slope of the regression line

Nominal thickness	Sample designation	n	m_E	b_E	S_F	S_ε	$S_{\varepsilon F}$	S_{mE}	r
		-	N	N	N	-	N	N	-
6.4 mm	6-1	141	450 683.3	10.2	207.6	0.000460	0.096	589.1	~1
	6-2	155	454 651.1	10.8	227.9	0.000501	0.114	378.7	~1
	6-3	144	440 306.9	12.4	211.9	0.000481	0.102	501.5	~1
8.4 mm	8-1	204	503 976.8	15.2	301.0	0.000597	0.180	451.0	~1
	8-2	167	479 961.9	15.5	246.1	0.000513	0.126	644.1	~1
	8-3	136	498 843.9	7.8	200.6	0.000402	0.081	445.3	~1
10.4 mm	10-1	179	726 046.8	12.9	265.1	0.000365	0.097	586.0	~1
	10-2	190	664 505.0	9.8	280.9	0.000423	0.119	400.1	~1
	10-3	186	628 277.5	12.7	274.7	0.000438	0.120	643.9	~1
12.4 mm	12-1	205	693 886.8	8.9	303.5	0.000437	0.133	593.1	~1
	12-2	282	742 740.1	21.8	417.3	0.000562	0.234	599.5	~1
	12-3	77	660 760.8	22.3	277.0	0.000419	0.116	1236	~1

Table 7. Young's modulus E with the measurement uncertainty (expansion coefficient k = 2)

Nominal thickness	Sample designation	m_E	S_{mE}	S_0	u_{S0}	E	u_E	$E \pm U_E$	$E \pm U_E$ (avg.)
		N	N	mm²	mm²	MPa	MPa	MPa	MPa
6.4 mm	6-1	450 683.3	589.1	65.5	1.8	6 883	188	6 883 ± 376	6 882 ± 590
	6-2	454 651.1	378.7	63.9	2.6	7 114	295	7 114 ± 590	
	6-3	440 306.9	501.5	66.2	2.6	6 650	261	6 650 ± 521	
8.4 mm	8-1	503 976.8	451.0	86.2	3.7	5 848	252	5 848 ± 504	5 760 ± 532
	8-2	479 961.9	644.1	85.8	4.1	5 594	266	5 594 ± 532	
	8-3	498 843.9	445.3	85.4	3.5	5 838	238	5 838 ± 475	
10.4 mm	10-1	726 046.8	586.0	110.7	4.0	6 561	236	6 561 ± 473	6 246 ± 472
	10-2	664 505.0	400.1	105.8	3.0	6 283	177	6 283 ± 354	
	10-3	62 8277.5	643.9	106.6	3.3	5 894	182	5 894 ± 363	
12.4 mm	12-1	693 886.8	593.1	126.1	4.1	5 501	180	5 501 ± 359	5 591 ± 390
	12-2	742 740.1	599.5	128.5	4.3	5 782	195	5 782 ± 389	
	12-3	660 760.8	1236	120.4	3.3	5 490	149	5 490 ± 298	

measurement uncertainties, are given in Table 4, Table 5 and Table 7. The uncertainty in the measurement of the average value of the strength parameter takes into account the scatter in the results obtained for the different thicknesses of the plates.

CDF wood-based boards have a high density of more than 1000 kg/m³. Their tensile strength of at least 27.1 MPa is greater than that of MDF boards: 20.7 MPa (tempered), 15.2 MPa (standard), 3.8 MPa (service-tempered) (Youngquist, 1999; Jakimovska Popovska, Iliev and Spiroski, 2016). CDF boards, like MDF and HDF boards, have a low total elongation at break of about 0.5%. They exhibit greater stiffness: their Young's modulus (at least 5,600 MPa) is greater than that of high-density (3,450 MPa) or medium-density panels (2,400 MPa). Wood-based boards containing melamine admixtures have been subjected to numerous tests. Lieber et al. (2018) analyzed the effect of the seasoning period of particleboards on their mechanical properties. For this purpose, particleboards were produced in laboratory conditions with a thickness of 16 mm and a density of 680 kg/m³, using melamine–urea–formaldehyde resin. Eight variants of board seasoning were tested. The highest value of the modulus of elasticity (3,017 MPa) was recorded for boards seasoned for 7 days, and the lowest (2,601 MPa) for unseasoned boards.

In turn, increasing the content of melamine paper has been shown to improve the mechanical properties of boards by reducing water absorption and board swelling. In a recent study, the lowest Young's modulus value (1,436 MPa) was obtained for boards without melamine. The addition of melamine paper significantly increased the value of this parameter to 1,729 MPa for a 5% melamine paper content and 1,884 MPa for a 10% content (Franco et al., 2024). The results of research on the influence of the conditions of use on selected properties of furniture chipboards finished with a melamine film showed that the values of the modulus of elasticity can range from about 3,400 to 4,000 MPa (Borysiuk et al., 2019).

The values of the modulus of elasticity obtained in our own studies are much higher. This indicates that CDF boards are much more difficult to deform.

The research results were subjected to statistical analysis. The first step was to perform the Shapiro–Wilk test. The null hypothesis of this test is that the population is normally distributed. If the p-value is greater than the chosen level of significance $\alpha = 0.05$, then the null hypothesis cannot be rejected. If the p-value is less than α, then the null hypothesis is rejected and there is evidence that the tested data are not normally distributed. Values of the Shapiro–Wilk test statistic *W* and p-values for each tested thickness of CDF panels are listed in Table 8. The results of the analysis show that in the case of tensile strength R_m and percentage total extension at fracture A_t, the assumption of normality of distribution is met. For these

Table 8. Results of conducting the Shapiro-Wilk test (α = 0.05)

Nominal thickness	R_m		A_t		E	
	Test statistic W	p-value	Test statistic W	p-value	Test statistic W	p-value
6.4 mm	0.9297	0.4876	0.9985	0.9265	0.9996	0.9620
8.4 mm	0.9908	0.8168	0.9951	0.8667	0.7669	0.0377
10.4 mm	0.9952	0.8679	0.9075	0.4098	0.9910	0.8184
12.4 mm	0.8710	0.2983	0.8297	0.1875	0.9995	0.9572

Table 9. Results of conducting the Levene's test and the Brown-Forsythe's test (α = 0.05)

Parameter	Levene's test		Brown-Forsythe's test	
	Test statistic F	p-value	Test statistic F	p-value
R_m	2.11	0.18	0.61	0.63
A_t	2.03	0.19	0.72	0.57
E	0.42	0.75	0.39	0.77

Table 10. Results of conducting the Bartlett's test, Cochran's test and the Hartley's test (α = 0.05)

Parameter	Bartlett's test	Cochran's test	Hartley's test	p-value
	Test statistic χ^2	Test statistic C	Test statistic F	
R_m	3.35	0.44	14.81	0.34
A_t	3.90	0.55	24.64	0.27
E	1.08	0.39	4.85	0.78

Table 11. Results of One-Way analysis of variance ANOVA (α = 0.05)

Parameter	One-Way ANOVA	
	Test statistic F	p-value
R_m	2.57	0.13
A_t	1.16	0.38

parameters, the next step was to check the assumption of homogeneity of variance.

Levene's test is used to assess the equality of variances for a variable calculated for two or more groups. Since the p-value obtained from Levene's test is greater than the significance level α = 0.05, the null hypothesis of the test indicates that the population variances are equal. An analogous conclusion follows from the other tests (Table 9 and Table 10). In this situation it is possible to perform one-way analysis of variance (ANOVA). Since the p-value resulting from one-way ANOVA is greater than the significance level α = 0.05, we accept the null hypothesis that there is no difference in the tensile strength R_m due to the thickness of the CDF plate. The same conclusion is indicated by the results of one-way ANOVA for percentage total extension at fracture A_t (Table 11).

Since for one thickness the Young's modulus E has a p-value less than the significance level of α = 0.05, and therefore the assumption of normality

Table 12. Results of the non-parametric Kruskal-Wallis test and the median test (α = 0.05)

Parameter	Kruskal-Wallis test		Median test	
	Test statistic H	p-value	Test statistic χ^2	p-value
E	9.97	0.0188	12.00	0.0074

of distribution was not met, the non-parametric Kruskal–Wallis test, for testing whether samples originate from the same distribution, was performed, as well as the median test. The p-values obtained in both tests (Table 12) are less than the significance level, indicating that the results of the tests for at least one thickness of CDF plate are significantly different from the others. To identify such a group of results, multiple comparison tests of sample mean ranks were performed. The analysis showed that the fourth group of results (for a CDF plate thickness of 12.4 mm) was the only one that differed significantly from the other groups ($p = 0.0195 < \alpha = 0.05$).

Conclusions

1. CDF boards are brittle materials for which it is not possible to determine a conventional yield strength.
2. Compared with classic MDF/HDF boards, the increased density and unique structure of CDF boards provide increased strength.
3. The strength of CDF wood-based boards does not depend on their thickness. Statistical analysis has shown that in the case of boards up to 12.4 mm thick, their thickness does not affect their strength properties. A difference was detected only in the value of Young's modulus for the largest tested thickness, 12.4 mm.
4. CDF boards, like MDF and HDF boards, exhibit low total elongation at break.
5. CDF boards are more rigid and less susceptible to deformation than HDF or MDF boards.
6. The described functional features and strength properties of CDF boards make them a very interesting material with a wider range of applications than their classic counterparts.

References

Arendarski J. (2013): Measurement uncertainty (in Polish). Warsaw: Publishing House of the Warsaw University of Technology.

Borysiuk P., Furmanik A., Auriga R., (2019): Impact of conditions of use on selected properties of furniture particleboards finished with melamine film. Biuletyn Informacyjny Ośrodka Badawczo-Rozwojowego Przemysłu Płyt Drewnopochodnych w Czarnej Wodzie. No. 3/4. pp. 107-117.

Franco M., Silva M.F., Prates G., Gali L., Savi A., Favarim H., Caraschi J., Campos C. (2024): Physical-mechanical properties of MDF panels with the addition of melaminę paper in the internal layer, Cadero Pedagogico. Vol. 21, No. 1, pp. 2992-3001.

Hunt J. F., Vick C.B. (1999): Strength and processing properties of wet-formed hardboards from recycled corrugated containers and commercial hardboard fibers. Forest Products Journal. 49(5), pp. 69-74.

Jakimovska Popovska V., Iliev B., Spiroski I. (2016): Characteristics of Medium Density Fiberboards for Furniture Production and Interior Application. South East European Journal of Architecture and Design, p. 10013.

Kim M.H., Song H.B. (2014): Analysys of the global warming potential for wood waste recycling systems. Journal of Cleaner Production, 69, pp. 199-207.

Kostyrko K., Piotrowski J. (2012): Calibration of measuring equipment (in Polish). Warsaw: PWN Scientific Publishing House.

Lieber E., Pawlak D., Boruszewski P. (2018): Analiza wpływu okresu sezonowania płyt wiórowych na ich właściwości mechaniczne. Biuletyn Informacyjny Ośrodka badawczo-Rozwojowego Przemysłu Płyt Drewnopochodnych w Czarnej Wodzie. No. 1/2, pp. 118-128.

Lubis M.A.R., Hong M.K., Park. B.D., Lee S.M. (2018):. Effects of recycled fiber content on the properties of medium density fiberboard. European Journal Wood and Wood Products. 76(6). pp. 1515-1526.

Md. Rowson A., Ummi Hani A., Zaidon A., Lee S.H., Norul Hisham H., Siti Hasnah K., (2022): Physical properties of hydrothermally treated rubberwood [Hevea brasiliensis (Willd. ex A. Juss.) Mull. Arg.] in Different Buffered Media. Forests, Vol. 13, No. 7, pp. 1-14.

Nourbakhsh A., Ashori A., Jahan-Latibari A. (2010): Evaluation of the physical and mechanical properties of medium density fiberboard made from old newsprint

fibers. Journal of Reinforced Plastics and Composites. 29(1), pp. 5-11.

Oniśko W. (2011): New generations of wood-based composites and modern technologies. In Proceeding of the Drewnowizja, Instytut Technologii Drewna w Poznaniu

Rabiej M. (2018): Statistical analysis with the programs Statistica and Excel (in Polish). Gliwice: Helion Publishing House.

Roila A., Noorshamsiana A. W., Zawawi I., Astimar A.A. (2023): Medium density fibreboard (MDF) from oil palm fibre: a review, Malaysian Journal of Analytical Sciences, Vol. 27, No. 3, pp. 626- 640.

Sala C. M., Robles E., Kowaluk G. (2020): Influence of adding offcuts and trims with a recycling approach on the properties of high-density fibrous composites. Polymers. Vol. 12(6).

StatSoft (2006): Elektroniczny Podręcznik Statystyki PL. Retrieved from https://www.statsoft.pl/textbook/stathome.html

Swiss Krono (2023). Catalog: SwissCDF innovatively furnishes interiors (in Polish). Swiss Krono.

Swiss Krono: Product card – MDF, LDF, HDF boards.

Sydor M., Wołpiuk M. (2016): Analysis of Resistance to Axial Withdrawal of Screws Embedded in Locally Reinforced MDF. Drewno, pp. Vol. 59, No. 196, pp. 173-182.

Youngquist J. A. (1999): Wood-based Composites and Panel Products. In F. P. Laboratory, Wood handbook: wood as an engineering material. General technical report FPL; GTR-113. Madison, WI: U.S. Department of Agriculture, Forest Service, Forest Products Laboratory.

Zhao J., Tian D., Shen F., Hu J., Zeng Y., Huang C. (2019): Valorizing waste lignocellulose-based furniture boards by phosphoric acid and hydrogen peroxide (Php) pretreatment for bioethanol production and high-value lignin recovery. Sustainability, 11, 6175.

List of standards

EN 310:1993 Wood-based panels – Determination of modulus of elasticity in bending and of bending strength.

PN-EN ISO 527-2:2012 Plastics – Determination of tensile properties, Part 2: test conditions for moulding and extrusion plastics.

PN EN ISO 3167:2014-09 Plastics – Multipurpose test specimens.